Alexandria Engineering Journal (2016) 55, 2107–2114

HOSTED BY

ELSEVIER

Alexandria University

Alexandria Engineering Journal

www.elsevier.com/locate/aej
www.sciencedirect.com

ORIGINAL ARTICLE

Velocity, thermal and concentration slip effects on a magneto-hydrodynamic nanofluid flow

M. Awais [a,*], **T. Hayat** [b], **Aamir Ali** [a], **S. Irum** [a]

[a] *Department of Mathematics, COMSATS Institute of Information Technology, Attock 43600, Pakistan*
[b] *Department of Mathematics, Quaid-I-Azam University, 45320 Islamabad 44000, Pakistan*

Received 28 May 2014; revised 19 May 2016; accepted 25 June 2016
Available online 9 August 2016

KEYWORDS

Slip conditions;
MHD;
Nanofluid;
Streamline analysis

Abstract This article examines the magneto-hydrodynamic (MHD) flow of nanofluid bounded by a stretching surface. The slip conditions are utilized in the present analysis. The involved differential systems are solved for the velocity, temperature and mass fraction. Graphical and numerical results are reported for the analysis of various parameters of interest entering into the modeled problems. Combined effects of thermal and concentration jump are analyzed. Various tables are constructed to show the rheological effects of different physical parameters. Streamlines are plotted showing the rheology for the slip and no slip flow regime. Plots of skin friction are also prepared for the slip and magnetic field effects.

1. Introduction

The study of boundary layer flows has stimulated considerable attention of scientists during the past five decades. This type of flows appears in various engineering applications such as polymer extrusion, continuous casting, glass fiber and paper production, food manufacturing, stretching of plastic films and several other processes. Crane [1] presented earliest study on the steady flow over a stretching sheet. He obtained the closed form solution. Now there is abundant literature available on the flow induced by a stretched surface under various aspects (see few recent studies [2–4]). It is argued that quality of final product in manufacturing processes largely depends upon the rate of cooling. Hence to control cooling system in such process is very important. The simultaneous effects of heat transfer and magnetohydrodynamic (MHD) are useful in order to achieve the final product of desire characteristics. Such considerations are very important especially in the metallurgical processes including the cooling of continuous strips and filaments drawn through a quiescent fluid and purification of molten metals from nonmetallic inclusions. The cooling rate is controlled by drawing the strips in an electrically conducting fluid subject to a magnetic field [5]. A broad description of the MHD/slip/heat transfer effects can be found for instance, to mention the few recent attempts in studies [6–15].

The word "nanofluid" introduced by Choi et al. [16] describes a liquid in which nanometer sized particles are suspended in conventional heat transfer basic fluid. It was noted by Masuda et al. [17] that nanofluids are characterized by enhanced thermal conductivity. No doubt, the conventional fluids used in heat transfer processes such as water, mineral oils and ethylene glycol have low thermal conductivity. Hence several techniques are adopted to improve the thermal

* Corresponding author.
E-mail address: awais_mm@yahoo.com (M. Awais).
Peer review under responsibility of Faculty of Engineering, Alexandria University.

http://dx.doi.org/10.1016/j.aej.2016.06.027

conductivity of such fluids by suspending nano/micro sized particle materials in liquids. Having this in mind, the literature in the mechanics of nanofluids is sizeable now (see [18,19] and many Refs. therein).

The goal of present communication is to venture further in the regime of nanofluids. Thus in this paper we investigate the simultaneous effects of magnetic field and slippage on the stagnation point flow of nanofluid over a stretching surface. The variations of Brownian motion and thermophoresis are particularly analyzed. The no-slip boundary condition (the assumption that a liquid adheres to a solid boundary) is frequently utilized in flow problems of viscous fluids. However, there are cases where such condition is inadequate and slip may occur on the boundary when the fluid is particulate such as emulsions, suspensions, foams and polymer solutions. The fluid flow behavior subject to the slip flow regime greatly differs from the traditional flow. The slip flows under different flow configurations have been studied by many researchers. The solutions are constructed by employing homotopy analysis method ([20–22] and studies mentioned in them). Plots are presented and examined. To the best of our knowledge, this is the first study dealing with slip effects on the flow of a nanofluid.

2. Mathematical analysis

We consider the flow near a stagnation point toward a stretching sheet. The nanofluid is over a stretching sheet. A uniform magnetic field of strength B_0 is applied normally to the stretched surface as shown in Fig. 1.

The temperature and concentration of sheet are denoted by T_w and C_w whereas T_∞ and C_∞ are the ambient values of temperature and concentration respectively. Induced magnetic field effect is not considered in view of small magnetic Reynolds number assumptions. Further, there are slippage effects. The dimensional boundary layer equations can be written as follows:

$$\frac{\partial u}{\partial x}+\frac{\partial v}{\partial y}=0, \tag{1}$$

$$u\frac{\partial u}{\partial x}+v\frac{\partial u}{\partial y}=u_e(x)\frac{du_e(x)}{dx}+\nu\frac{\partial^2 u}{\partial y^2}+\frac{\sigma B_0^2}{\rho_f}(u_e-u) \tag{2}$$

$$u\frac{\partial T}{\partial x}+v\frac{\partial T}{\partial y}=\alpha_m\frac{\partial^2 T}{\partial y^2}+\frac{(\rho c)_p}{(\rho c)_f}\left\{D_B\frac{\partial C}{\partial y}\frac{\partial T}{\partial y}+\frac{D_T}{T_\infty}\left(\frac{\partial T}{\partial y}\right)^2\right\} \tag{3}$$

$$u\frac{\partial C}{\partial x}+v\frac{\partial C}{\partial y}=D_B\frac{\partial^2 C}{\partial y^2}+\frac{D_T}{T_\infty}\frac{\partial^2 T}{\partial y^2} \tag{4}$$

with the following boundary conditions:

$$\begin{aligned} &u=u_w(x)+\gamma_1\frac{\partial u}{\partial y},\quad v=0,\ T=T_w+\gamma_2\frac{\partial T}{\partial y},\\ &C=C_w+\gamma_3\frac{\partial C}{\partial y}\ \text{at}\ \ y=0,\\ &u=u_e(x),\quad v=0,\ T\to T_\infty,\ C\to C_\infty\ \text{as}\ \ y\to\infty, \end{aligned} \tag{5}$$

in which $u_w(x)=cx$ is the velocity of the stretching surface and $u_e(x)=ax$ is the free stream velocity far away from the stretching surface. Moreover the velocity components (u and v) are along x- and y-axes respectively, ν the kinematic viscosity, T_w the wall temperature, C_w concentration of species near the surface, T_∞ the ambient temperature, C_∞ ambient concentration, σ the electrical conductivity, B_0 the constant magnetic field, p the pressure, D_B the Brownian diffusion coefficient, ρ_f the fluid density, D_T the thermophoretic diffusion coefficient, α_m the thermal diffusivity, $(\rho c)_p$ the effective heat capacity of the nanoparticle material, $(\rho c)_f$ the heat capacity of the fluid and $(\gamma_1,\gamma_2,\gamma_3)$ the slip parameters for velocity, temperature and concentration respectively.

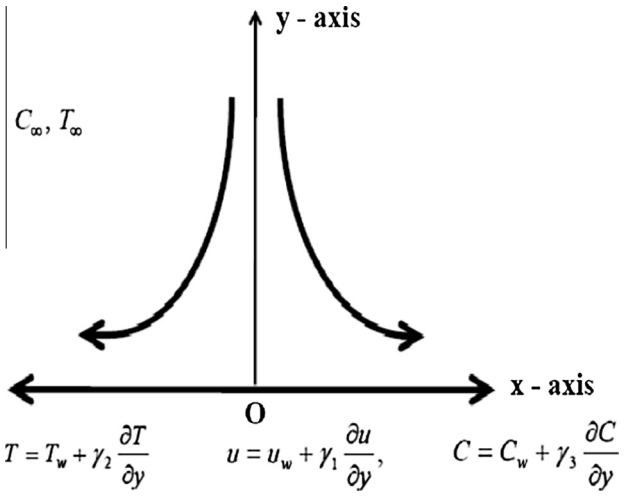

Figure 1 Geometry of the problem.

By introducing

$$\begin{aligned} &\eta=\sqrt{\frac{c}{\nu}}\,y,\quad u=cxf'(\eta),\ v=-\sqrt{c\nu}f(\eta),\\ &\theta(\eta)=\frac{T-T_\infty}{T_w-T_\infty},\quad \phi(\eta)=\frac{C-C_\infty}{C_w-C_\infty} \end{aligned} \tag{6}$$

Eq. (1) is satisfied identically and Eqs. (2–5) take the following forms:

$$f'''-(f')^2+ff''+A^2-M^2(f'-A)=0, \tag{7}$$

$$\theta''+\Pr(f\theta'+N_b\phi'\theta'+N_t(\theta')^2)=0, \tag{8}$$

$$\phi''+Lef\phi'+\frac{N_t}{N_b}\theta''=0, \tag{9}$$

$$\begin{aligned} &f(0)=0,\quad f'(0)-S_1f''(0)=1,\\ &\theta(0)-S_2\theta'(0)=1,\ \phi(0)-S_3\phi'(0)=1,\\ &f'(\infty)=A,\ \theta(\infty)=0,\ \phi(\infty)=0. \end{aligned} \tag{10}$$

The quantities $A=\frac{a}{c}$ denote the stretching ratio, M the magnetic parameter, $Le=\frac{\nu}{D_B}$ the Lewis number, $\Pr=\frac{\nu}{\alpha_m}$ the Prandtl number, $N_b=\frac{(\rho c)_p D_B(\phi_w-\phi_\infty)}{(\rho c)_f\nu}$ the Brownian motion parameter, $N_t=\frac{(\rho c)_p D_T(T_w-T_\infty)}{(\rho c)_f T_\infty\nu}$ the thermophoresis parameter, $S_1=\gamma_1\sqrt{c/\nu}$ the velocity slip, $S_2=\gamma_2\sqrt{c/\nu}$ the thermal slip and $S_3=\gamma_3\sqrt{c/\nu}$ the concentration slip.

The Nusselt number Nu and Sherwood number Sh are respectively given by

$$Nu=\frac{xq_w}{k(T_w-T_\infty)},\quad Sh=\frac{xq_m}{D_B(C_w-C_\infty)},$$

in which q_w and q_m denote the surface heat flux and surface mass flux respectively. In dimensionless form

$$Nu/Re_x^{1/2}=-\theta'(0),\ Sh/Re_x^{1/2}=-\phi'(0),$$

where $Re_x=cx/\nu$ denotes the Reynolds number.

3. Homotopy Analysis Method (HAM)

Homotopy analysis method is employed to compute the solution of Eqs. (7–9). By using the set of base functions

$$\{\eta^k \exp(-n\eta) | k \geqslant 0, n \geqslant 0\}, \tag{11}$$

one can express

$$f(\eta) = a_{0,0}^0 + \sum_{n=0}^{\infty}\sum_{k=0}^{\infty} a_{m,n}^k \eta^k \exp(-n\eta), \tag{12}$$

$$\theta(\eta) = \sum_{n=0}^{\infty}\sum_{k=0}^{\infty} b_{m,n}^k \eta^k \exp(-n\eta), \tag{13}$$

$$\phi(\eta) = \sum_{n=0}^{\infty}\sum_{k=0}^{\infty} c_{m,n}^k \eta^k \exp(-n\eta), \tag{14}$$

where $a_{m,n}^k$, $b_{m,n}^k$ and $c_{m,n}^k$ are the coefficients. Through rule of solution expressions and the boundary conditions (10), the initial guesses f_0, θ_0 and ϕ_0 of $f(\eta)$, $\theta(\eta)$ and $\phi(\eta)$ are chosen in the following form:

$$f_0(\eta) = 1 - \exp(-\eta), \tag{15}$$

$$\theta_0(\eta) = \exp(-\eta), \tag{16}$$

$$\phi_0(\eta) = \exp(-\eta), \tag{17}$$

whereas the auxiliary linear operators are

$$L_f = \frac{d^3 f}{d\eta^3} - \frac{df}{d\eta}, \tag{18}$$

$$L_\theta = \frac{d^2\theta}{d\eta^2} - \theta, \tag{19}$$

$$L_\phi = \frac{d^2\phi}{d\eta^2} - \phi, \tag{20}$$

with

$$L_f[C_1 + C_2 \exp(\eta) + C_3 \exp(-\eta)] = 0, \tag{21}$$

$$L_\theta[C_4 \exp(\eta) + C_5 \exp(-\eta)] = 0, \tag{22}$$

$$L_\phi[C_6 \exp(\eta) + C_7 \exp(-\eta)] = 0, \tag{23}$$

and $C_i (i = 1 - 7)$ are the arbitrary constants.

Denoting $p \in [0, 1]$ as the embedding parameter and $\hbar_f$, $\hbar_\theta$ and $\hbar_\phi$ the non-zero auxiliary parameters, the zeroth order deformation problems are constructed by the following expressions:

$$(1-p)L_f[\hat{f}(\eta,p) - f_0(\eta)] = p\hbar_f N_f[\hat{f}(\eta,p)], \tag{24}$$

$$(1-p)L_\theta[\hat{\theta}(\eta,p) - \theta_0(\eta)] = p\hbar_\theta N_\theta[\hat{\theta}(\eta,p)], \tag{25}$$

$$(1-p)L_\phi[\hat{\phi}(\eta,p) - \phi_0(\eta)] = p\hbar_\phi N_\phi[\hat{\phi}(\eta,p)], \tag{26}$$

where the non-linear operators N_f, N_θ and N_ϕ are as follows:

$$N_f[\hat{f}(\eta,p)] = \frac{\partial^3 \hat{f}(\eta,p)}{\partial\eta^3} - M^2 \frac{\partial \hat{f}(\eta,p)}{\partial\eta} - \left(\frac{\partial \hat{f}(\eta,p)}{\partial\eta}\right)^2 + \hat{f}(\eta,p)\frac{\partial^2 \hat{f}(\eta,p)}{\partial\eta^2} + A^2 + M^2 A, \tag{27}$$

$$N_\theta[\hat{f}(\eta,p), \hat{\theta}(\eta,p), \hat{\phi}(\eta,p)] = \frac{\partial^2\hat{\theta}(\eta,p)}{\partial\eta^2} + \Pr\left(\hat{f}(\eta,p)\frac{\partial\hat{\theta}(\eta,p)}{\partial\eta} + N_b \frac{\partial\hat{\theta}(\eta,p)}{\partial\eta}\frac{\partial\hat{\phi}(\eta,p)}{\partial\eta} + N_b \frac{\partial^2\hat{\theta}(\eta,p)}{\partial\eta^2}\right), \tag{28}$$

$$N_\phi[\hat{f}(\eta,p), \hat{\theta}(\eta,p), \hat{\phi}(\eta,p)] = \frac{\partial^2\hat{\phi}(\eta,p)}{\partial\eta^2} + Le\hat{f}(\eta,p)\frac{\partial\hat{\phi}(\eta,p)}{\partial\eta} + \frac{N_b}{N_t}\frac{\partial^2\hat{\theta}(\eta,p)}{\partial\eta^2}, \tag{29}$$

when $p = 0$ and $p = 1$ then

$$\hat{f}(\eta,0) = f_0(\eta),\ \hat{f}(\eta,1) = f(\eta), \tag{30}$$

$$\hat{\theta}(\eta,0) = \theta_0(\eta),\ \hat{\theta}(\eta,1) = \theta(\eta), \tag{31}$$

$$\hat{\phi}(\eta,0) = \phi_0(\eta),\ \hat{\phi}(\eta,1) = \phi(\eta), \tag{32}$$

and now utilizing Taylor series, we have

$$\hat{f}(\eta,p) = f_0(\eta) + \sum_{m=1}^{\infty} f_m(\eta)p^m, \tag{33}$$

$$\hat{\theta}(\eta,p) = \theta_0(\eta) + \sum_{m=1}^{\infty} \theta_m(\eta)p^m, \tag{34}$$

$$\hat{\phi}(\eta,p) = \phi_0(\eta) + \sum_{m=1}^{\infty} \phi_m(\eta)p^m, \tag{35}$$

$$f_m(\eta) = \frac{1}{m!}\frac{\partial^m f(\eta,p)}{\partial p^m}\bigg|_{p=0},\quad \theta_m(\eta) = \frac{1}{m!}\frac{\partial^m \theta(\eta,p)}{\partial p^m}\bigg|_{p=0},$$
$$\phi_m(\eta) = \frac{1}{m!}\frac{\partial^m \phi(\eta,p)}{\partial p^m}\bigg|_{p=0}. \tag{36}$$

The auxiliary parameters are so properly chosen that the series (33)–(35) converge at $p = 1$ and hence

$$f(\eta) = f_0(\eta) + \sum_{m=1}^{\infty} f_m(\eta), \tag{37}$$

$$\theta(\eta) = \theta_0(\eta) + \sum_{m=1}^{\infty} \theta_m(\eta), \tag{38}$$

$$\phi(\eta) = \phi_0(\eta) + \sum_{m=1}^{\infty} \phi_m(\eta). \tag{39}$$

The corresponding deformation problems at the mth order are

$$L_f[f_m(\eta) - \chi_m f_{m-1}(\eta)] = \hbar_f R_m^f(\eta), \tag{40}$$

$$L_\theta[\theta_m(\eta) - \chi_m \theta_{m-1}(\eta)] = \hbar_\theta R_m^\theta(\eta), \tag{41}$$

$$L_\phi[\phi_m(\eta) - \chi_m \phi_{m-1}(\eta)] = \hbar_\phi R_m^\phi(\eta), \tag{42}$$

$$f_m(0) = 0,\ f_m'(0) = 0,\ f_m'(\infty) = 0,$$
$$\theta_m(0) = 0,\ \theta_m(\infty) = 0,$$
$$\phi_m(0) = 0,\ \phi_m(\infty) = 0, \tag{43}$$

$$R_m^f(\eta) = f_{m-1}''' + \sum_{k=0}^{m-1}\left[f_{m-1-k}f_k'' - f_{m-1-k}'f_k'\right] - M^2 f_{m-1}' + A^2 + M^2 A, \tag{44}$$

$$R_m^{\theta}(\eta) = \theta''_{m-1} + \Pr\sum_{k=0}^{m-1}\left[f_{m-1-k}\theta'_k + N_b\phi'_{m-1-k}\theta'_k + N_t\theta'_{m-1-k}\theta'_k\right], \quad (45)$$

$$R_m^{\phi}(\eta) = \phi''_{m-1} + Le\sum_{k=0}^{m-1}\left[f_{m-1-k}\phi'_k\right] + \frac{N_t}{N_b}\theta''_{m-1}. \quad (46)$$

The general solutions of Eqs. (44)–(46) can be written as

$$f_m(\eta) = f_m^*(\eta) + C_1 + C_2\exp(\eta) + C_3\exp(-\eta), \quad (47)$$

$$\theta_m(\eta) = \theta_m^*(\eta) + C_4\exp(\eta) + C_5\exp(-\eta), \quad (48)$$

$$\phi_m(\eta) = \phi_m^*(\eta) + C_6\exp(\eta) + C_7\exp(-\eta), \quad (49)$$

in which $f_m^*(\eta)$, $\theta_m^*(\eta)$ and $\phi_m^*(\eta)$ denote the special solutions and

$$\begin{aligned} &C_2 = C_4 = C_6 = 0,\\ &C_1 = -C_3 - f_m^*(0), C_3 = \left.\frac{\partial f^*(\eta)}{\partial\eta}\right|_{\eta=0},\\ &C_5 = -\phi_m^*(0), C_7 = -\theta_m^*(0). \end{aligned} \quad (50)$$

Thus we have prepared a table showing the convergence of the results. It is noted that convergent solutions are obtained for $\hbar_f$, $\hbar_\theta$ and $\hbar_\phi = -1.0$ as shown in Table 1.

4. Discussion

Here Figs. 2–14 are plotted to examine the effects of physical parameters on the velocity, temperature and mass fraction fields respectively. Figs. 2 and 3 present the streamline analysis for no-slip and slippage characteristics. It is noted that the rheology is quite different in both cases. Moreover the magnitude of velocity of an boundary layer is also quite different in both cases. Impact of A on the dimensionless velocity f' is revealed in Fig. 4. This Figure demonstrates that an increase in A yields an increase in velocity. Thus higher values of A with the larger free stream velocity result in the increase of the fluid velocity. Fig. 5 shows the magnetic field effects M on f'. It is found that velocity decreases when M is increased. Physically magnetic field together with slip effect acts as a retarding force. This retarding force can control the fluid's velocity which is useful in numerous applications such as magneto-hydrodynamic power generation and electromagnetic coating of wires and metal. The expected consequences of slip parameter are displayed in Fig. 6. It is noted that slip parameter decreases the velocity in the vicinity of boundary. Figs. 7–12 plot the variations of the Brownian motion parameter N_b, thermophoresis parameter N_t, thermal slip S_2 and concentration slip S_3 on the temperature profile θ and the mass fraction field ϕ respectively. The effects of N_b and N_t on the temperature θ are quite similar (Figs. 7 and 8) whereas an increase in N_t causes a rapid increase in mass fraction field ϕ. Fig. 10 shows that mass fraction field ϕ decreases when N_b increases. Influence of S_2 on temperature field θ is sketched in Fig. 11. This Figure depicts that thermal slip causes a reduction in the temperature field. The influence of S_3 on the mass fraction field is quite similar to that of S_2 on the temperature field as shown in Fig. 12. It is due to the fact that slip basically retards the fluid motion which finally shows a decrease in net molecular movement. Consequently less molecular movement decreases both

Table 1 Convergence table.

Order of approximation	$-f''(0)$	$-\theta'(0)$	$-\varphi'(0)$
1	0.443250	0.370000	0.230000
5	0.445480	0.303036	0.196150
10	0.445489	0.296311	0.186514
15	0.445489	0.295766	0.185378
20	0.445489	0.295711	0.185280
25	0.445489	0.295705	0.185273
30	0.445489	0.295705	0.185273
40	0.445489	0.295705	0.185273
50	0.445489	0.295705	0.185273

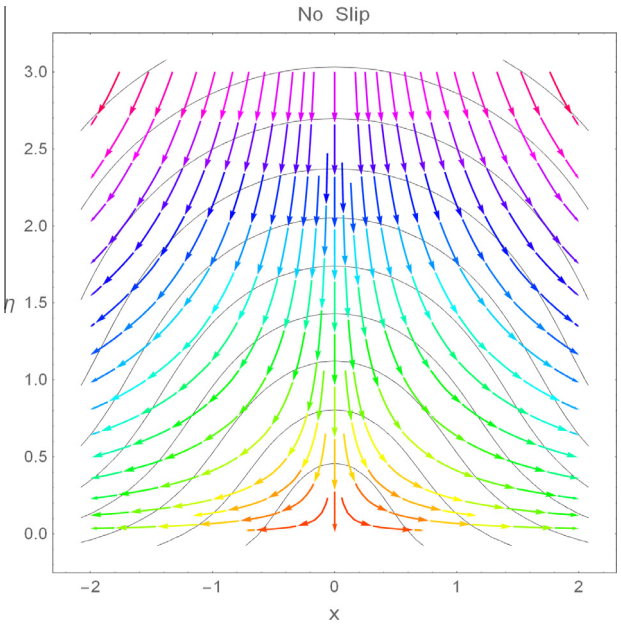

Figure 2 Streamlines for no-slip.

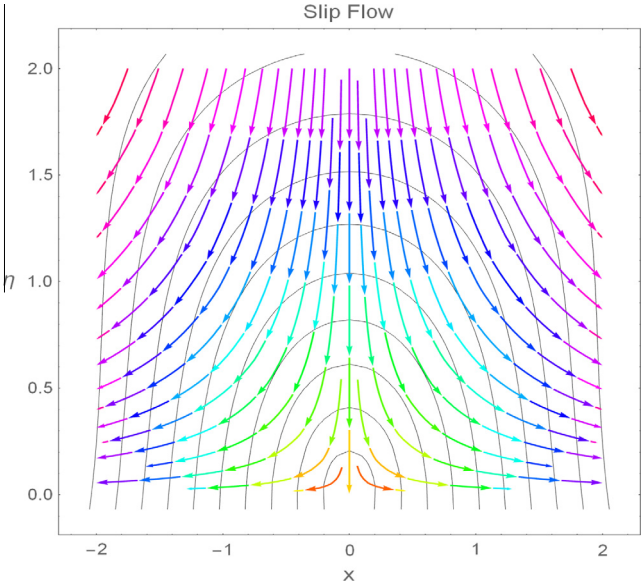

Figure 3 Streamlines for slippage.

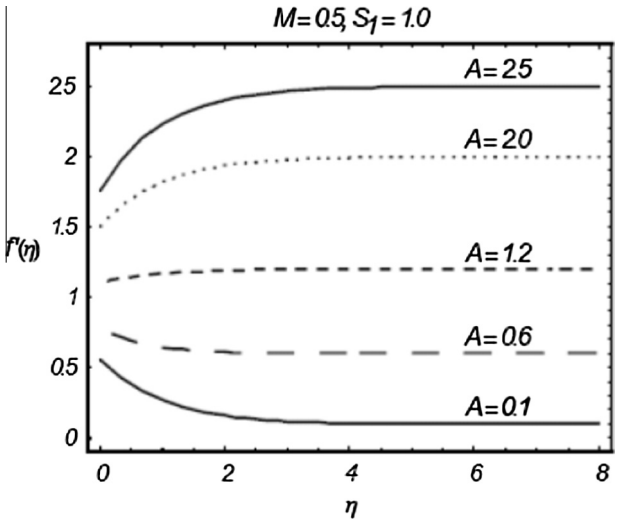

Figure 4 Influence of A on f'.

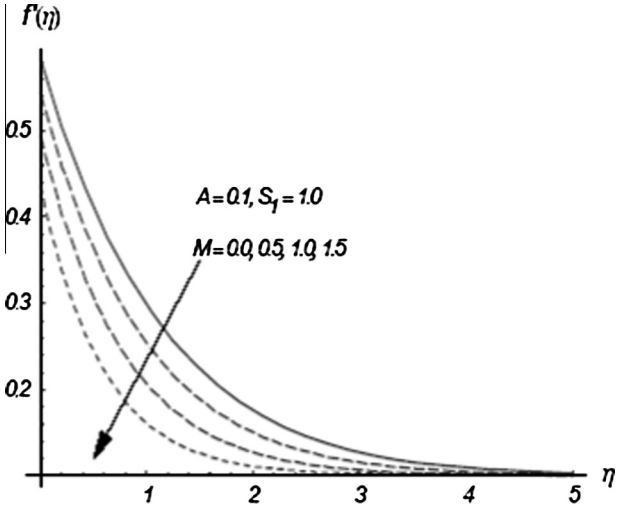

Figure 5 Influence of M on f'.

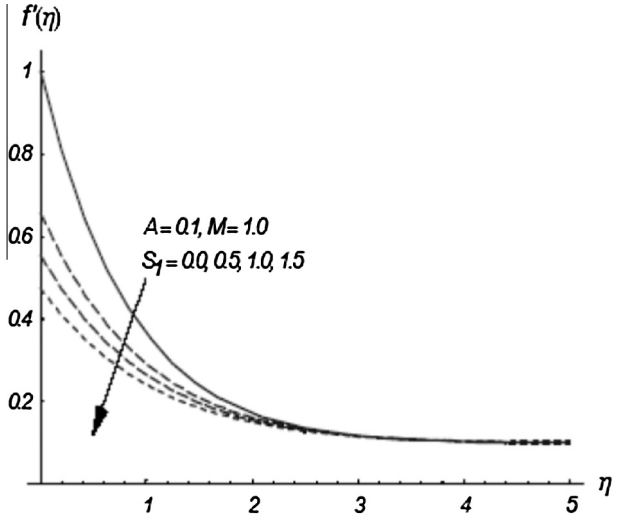

Figure 6 Influence of S_1 on f'.

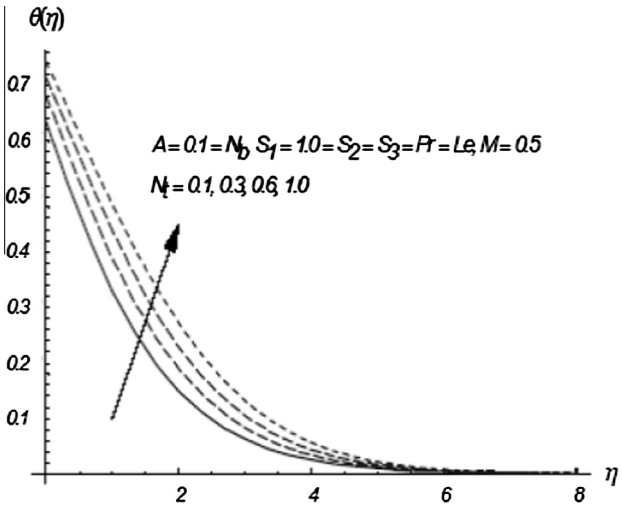

Figure 7 Influence of N_t on θ.

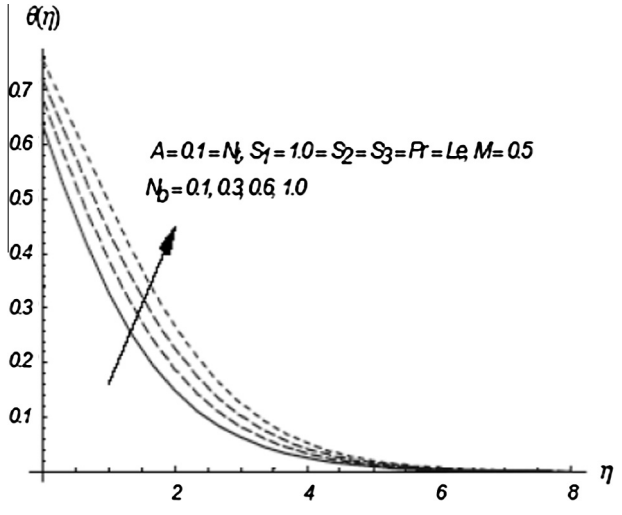

Figure 8 Influence of N_b on θ.

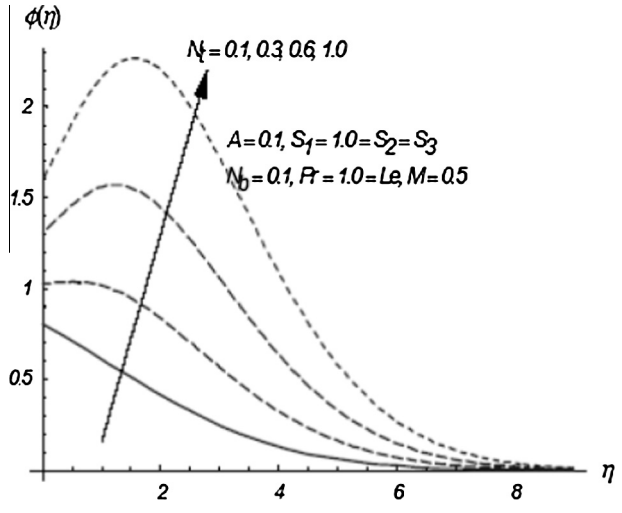

Figure 9 Influence of N_t on ϕ.

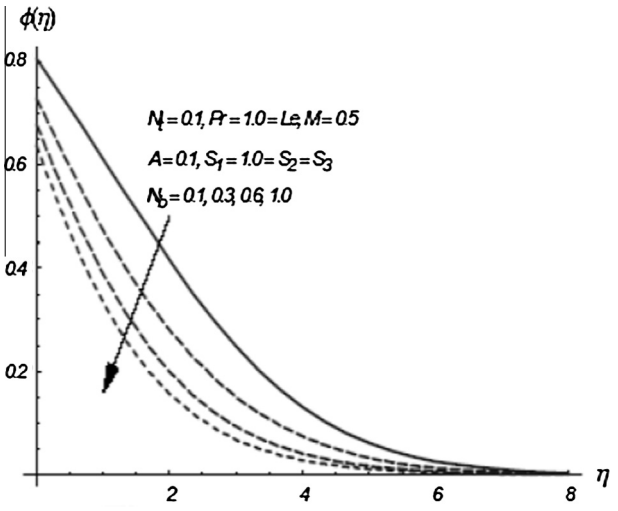

Figure 10 Influence of N_b on ϕ.

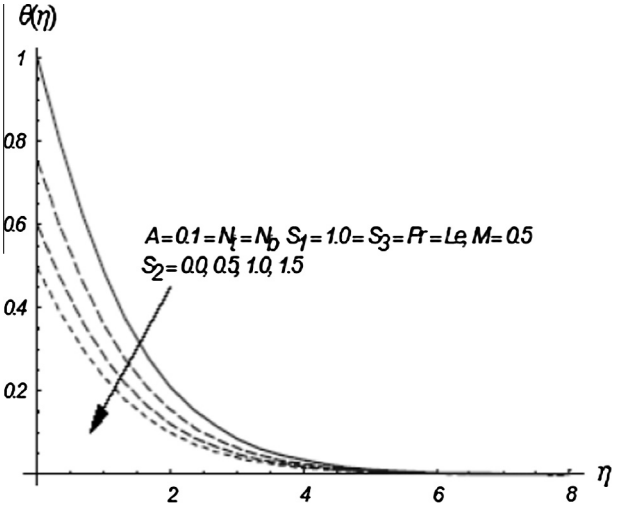

Figure 11 Influence of S_2 on θ.

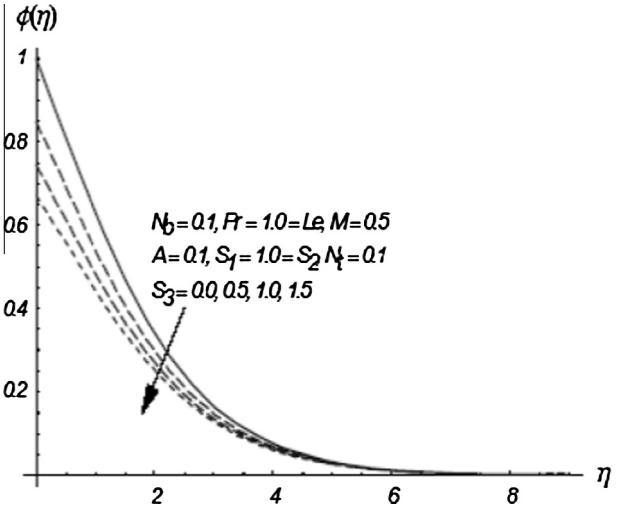

Figure 12 Influence of S_3 on θ.

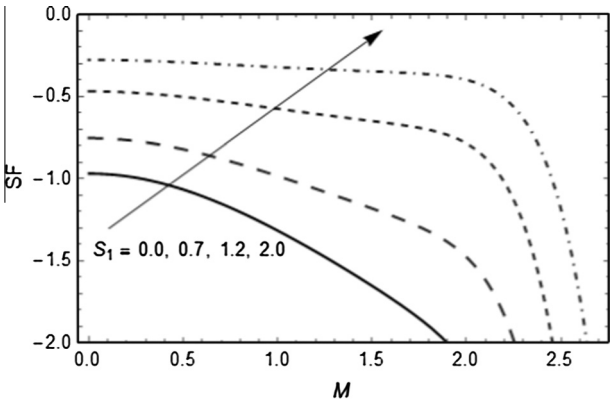

Figure 13 Influence of S_1 on skin friction against M.

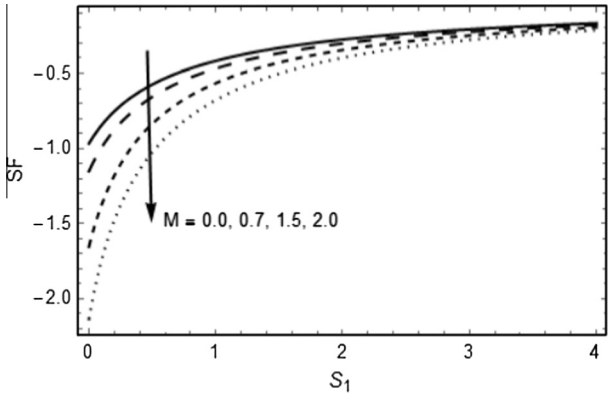

Figure 14 Influence of M on skin friction against S_1.

Table 2 Values of $Nu/Re_x^{1/2}$ and $Sh/Re_x^{1/2}$ for different values of A, M, N_b and N_t when $Pr = 1.0 = Le$ and $S_1 = 1.0 = S_2 = S_3$.

A	M	N_b	N_t	$Nu/Re_x^{1/2}$	$Sh/Re_x^{1/2}$
0.0	0.5	0.1	0.1	0.26929	0.14474
0.2	0.5	0.1	0.1	0.31739	0.21195
0.4	0.5	0.1	0.1	0.35272	0.25178
0.1	0.0	0.1	0.1	0.30729	0.19516
0.1	0.5	0.1	0.1	0.29570	0.18527
0.1	1.0	0.1	0.1	0.27173	0.16715
0.1	0.5	0.1	0.1	0.29570	0.18527
0.1	0.5	0.2	0.1	0.28845	0.24963
0.1	0.5	0.3	0.1	0.28125	0.27103
0.1	0.5	0.1	0.1	0.29570	0.18527
0.1	0.5	0.1	0.2	0.28984	0.06907
0.1	0.5	0.1	0.3	0.27419	−0.03954

temperature and mass fraction fields. Since if the thermal slip parameter can control the temperature inside the flow then it is quite possible the mass transport phenomenon can be controlled by the concentration slip parameter. Thus we have also analyzed the combined effects of velocity, thermal and concentration slip parameters on the flow. Quite interestingly we have found that the effects of concentration slip parameter are quite similar to those of thermal slip parameter. Conclusively one can control the thermal and concentration boundary layer

Table 3 Comparison table for skin friction when $S_1 = 0$ and $k_1 = M^2$.

M	Hamad and Ferdows [23]	Alsaedi et. al. [24]	Present
0.0	1.9991	1.9991	1.9991
0.1	2.0101	2.0101	2.0101
0.5	2.1102	2.1102	2.1102
1.0	2.3902	2.3902	2.3902

Table 4 Comparison of values for reduced Nusselt number $-\theta'(0)$.

Pr	Wang [25]	Khan and Pop [18]	Present
0.07	0.0656	0.0663	0.0663
0.20	0.1691	0.1691	0.1691
0.7	0.4539	0.4534	0.4534
2.0	0.9114	0.9113	0.9113
7.0	1.8454	1.8954	1.8954
20.0	3.3539	3.3539	3.3539
70.0	6.4622	6.4621	6.4621

Table 5 Thermo-physical properties of water and nanoparticles.

	ρ/kg·m^{-3}	C_p/J·kg^{-1}·K	k/W·m^{-1}·K	$\beta \times 10^5$/K^{-1}
Water	991.1	4179	0.613	21
Copper (Cu)	8933	385	401	1.67
Alumina (Al_2O_3)	3970	765	40	0.85
Silver (Ag)	10,500	235	429	1.89
Titanium Oxide (TiO_2)	4250	686.2	8.9538	0.9

up to the desired values by adjusting the thermal and concentration slip parameters.

In Fig. 13, the skin friction is plotted against magnetic field parameter M for various values of slip parameter S_1. It is observed that the skin friction increases for increasing S_1. From Fig. 14, we can also observe that the skin friction coefficient decreases with increasing M. Thus, the magnetic field reduces the friction at the wall.

Table 2 is constructed to show the numerical values of local Nusselt number $Re_x^{-1/2}Nu$ and Sherwood number $Re_x^{-1/2}Sh$ for different parametric values. Clearly, an increase in A leads to an increase in local Nusselt number whereas M, N_b and N_t show a decrease in the magnitude of local Nusselt number. Further, the magnitude of Sherwood number increases for positive values of A and N_b and decreases by increasing the values of M and N_t.

Table 3 shows the comparison of different values of skin friction with the published work when $S_1 = 0$ and $k_1 = M^2$.

Table 4 shows the comparison of different values of reduced Nusselt number $-\theta'(0)$ with the published work (see Table 5).

Acknowledgments

We sincerely thank the editor and the referees for the comments regarding improvement of our work.

References

[1] L.J. Crane, Flow past a stretching plate, ZAMP 21 (1970) 645–647.
[2] B. Yao, J. Chen, Series solution to the Falkner-Skan equation with stretching boundary, Appl. Math. Comput. 208 (2009) 156–164.
[3] T. Fang, J. Zhang, S. Yao, A new family of unsteady boundary layers over a stretching surface, Appl. Math. Comput. 217 (2010) 3747–3755.
[4] O.D. Makinde, W.M. Charles, Computational dynamics of hydromagnetic stagnation flow towards a stretching sheet, Appl. Comput. Math. 9 (2010) 243–251.
[5] C.H. Chen, Magneto-hydrodynamic mixed convection of a power-law fluid past a stretching surface in the presence of thermal radiation and internal heat generation/absorption, Int. J. Non-Linear Mech. 44 (2009) 596–603.
[6] K. Bhanttacharya, S. Mukhpadhyay, G.C. Layek, Steady boundary layer slip flow and heat transfer over a flat porous plate embedded in a porous media, J. Petrol. Sci. Eng. 78 (2011) 304–309.
[7] O.D. Makinde, P. Sibanda, Effects of chemical reaction on boundary layer flow past a vertical stretching surface in the presence of internal heat generation, Int. J. Numer. Meth. Heat Fluid Flow 21 (2011) 779–792.
[8] O.D. Makinde, W.M. Charles, Computational dynamics of hydromagnetic stagnation flow towards a stretching sheet, Appl. Comput. Math. 9 (2010) 243–251.
[9] T. Fang, S. Yao, I. Pop, Flow and heat transfer over a generalized stretching/shrinking wall problem–exact solutions of the Navier-Stokes equations, Int. J. Non-Linear Mech. 46 (2011) 1116–1127.
[10] M.M. Rashidi, S.A.M. Pour, Analytic approximate solutions for unsteady boundary-layer flow and heat transfer due to a stretching sheet by homotopy analysis method, Nonlinear Anal.: Model. Control 15 (2010) 83–95.
[11] J. Raza, A.M. Rohni, Z. Omar, M. Awais, Heat and mass transfer analysis of MHD nanofluid in a rotating channel with slip effects, J. Mol. Liq. 219 (2016) 703–708.
[12] M. Turkyilmazoglu, Heat and mass transfer of MHD second order slip flow, Comput. Fluids 71 (2013) 426–434.
[13] N.S. Akbar, Z.H. Khan, Heat transfer analysis of the peristaltic instinct of biviscosity fluid with the impact of thermal and velocity slips, Int. Commun. Heat Mass Transf. 58 (2014) 193–199.
[14] T. Hayat, M. Awais, A.A. Hendi, Three-dimensional rotating flow between two porous wall with slip and hat transfer, Int. Commun. Heat Mass Transf. 39 (2012) 551–555.
[15] M.G. Reddy, Heat and mass transfer on magnetohydrodynamic peristaltic flow in a porous medium with partial slip, Alex. Eng. J. 55 (2) (2016) 1225–1234.
[16] S.U.S. Choi, Z.G. Zhang, W. Yu, F.E. Lockwood, E.A. Grulke, Anomalously thermal conductivity enhancement in nanotube suspensions, Appl. Phys. Lett. 79 (2001) 2252–2254.
[17] H. Masuda, A. Ebata, K. Teramae, N. Hishinuma, Alteration of thermal conductivity and viscosity of liquids by dispersing ultra-fine particles, Netsu Bussei 7 (1993) 227–233.
[18] W.A. Khan, I. Pop, Boundary-layer flow of a nanofluid past a stretching sheet, Int. J. Heat Mass Transf. 53 (2010) 2477–2483.
[19] O.D. Makinde, A. Aziz, Boundary layer flow of a nanofluid past a stretching sheet with a convective boundary condition, Int. J. Therm. Sci. 50 (2011) 1326–1332.
[20] S. Abbasbandy, A. Shirzadi, A new application of the homotopy analysis method: solving the Sturm-Liouville problems, Commun. Nonlinear Sci. Numer. Simul. 16 (2011) 112–126.
[21] M.M. Rashidi, G. Domairry, S. Dinarvand, Approximate solutions for the Burger and regularized long wave equations

by means of the homotopy analysis method, Commun. Nonlinear Sci. Numer. Simul. 14 (2009) 708–717.
[22] T. Hayat, Ambreen Safdar, M. Awais, S. Mesloub, Soret and Dufour effects for three-dimensional flow in a viscoelastic fluid over a stretching surface, Int. J. Heat Mass Transf. 55 (2012) 2129–2136.
[23] M.A.A. Hamad, M. Ferdows, Similarity solution of boundary layer stagnation-point flow towards a heated stretching sheet saturated with a nanofluid with heat absorption/generation and suction/blowing: a lie group analysis, Commun. Nonlinear Sci. Numer. Simul. 17 (2012) 132–140.
[24] A. Alsaedi, M. Awais, T. Hayat, Effects of heat generation/absorption on stagnation point flow of nanofluid over a surface with convective boundary conditions, Commun. Nonlinear Sci. Numer. Simul. 17 (2012) 4210–4223.
[25] C.Y. Wang, Free convection on a vertical stretching surface, J. Appl. Math. Mech. (ZAMM) 69 (1989) 418–420.